This is a repository copy of *Micro-damage evolution and macro-mechanical property degradation of limestone due to chemical effects*.

White Rose Research Online URL for this paper:
http://eprints.whiterose.ac.uk/135667/

Version: Accepted Version

# Micro-damage evolution and macro-mechanical property degradation of limestone due to chemical effects

Hao Li [a,b,c], Zuliang Zhong[a,b,*], Yong Sheng[c], Xinrong Liu[a,b], Dongmin Yang[c,*]

[a] School of Civil Engineering, University of Chongqing, Chongqing, 400044, China

[b] National Joint Engineering Research Center of Geohazard Prevention in Reservoir Area, Chongqing University, Chongqing 400045, China

[c] School of Civil Engineering, University of Leeds, Leeds, LS2 9JT, UK

*corresponding authors. Email address: D.Yang@leeds.ac.uk; haiou983@126.com

## Abstract

In this study Nuclear Magnetic Resonance (NMR) imaging in combination with mechanical tests are carried out to investigate the influence of chemical solutions on porosity change, micro damage and macro mechanical property degradation of limestone samples under external stress. The NMR images and $T_2$ values for compression stage, micro damages emergence stage, micro damages development stage and fracture and collapse stage are obtained and analysed. The results of the corrosive influence of chemical solutions with different pH values and immersion periods on the mechanical property degradation of limestone samples are investigated. By choosing porosity as the damage variable, the micro damage of the samples during chemical erosion and triaxial compression are calculated. It can be concluded that pH values of the chemical solutions change the porosity and micro damage of the rock, which is the root reason for its mechanical properties degradation. The chemical erosion also has a significant influence on the micro crack propagation in the limestone samples under triaxial compression.

**Key words:** Nuclear Magnetic Resonance (NMR); $T_2$ spectrum distribution; Micro damage; Chemical effects; Limestone.

## 1 Introduction

Underground rock mass is often surrounded by water, containing complex chemical icons and different pH values, which may have complex effects on the mechanical properties of the underground rocks [1]. This is because the presence of water often contains different chemicals, and the reaction between chemical icons with rock is a significant factor that accelerates failure progress, leads to mechanical characteristics decrease of rock, or causes geological disasters, such

as land slope and earthquakes [2-4]. In underground storage constructions, such as nuclear waste storage [5, 6] and underground reservoirs [7], the water has a significant influence on the stability of these underground constructions. Research on mechanical properties of chemical corroded rock is one of the important topics in ground water reservoirs, oil drilling, $CO_2$ injection, toxic material or nuclear waste disposal, slope and dam foundation and underground rock engineering structures, *etc*.

Over the past few years, efforts have been made to investigate the mechanical response of the rocks to chemical effects, in particular the injection of $CO_2$ into sedimentary rocks [8-11]. Grgic et al., [12] conducted $CO_2$ injection tests on oolitic limestone in triaxial cells at temperature and mechanical stresses. The long-term mechanical and petrographical evolutions of the oolitic limestone were studied by a specific "flow-through" triaxial cell which can measure very low strain rates in both axial and lateral directions. Results indicate that $CO_2$ did not play a significant role in the chemistry of carbonate reservoirs due to the $H_2O$-$CO_2$-calcite re-equilibrium and did not induce reservoir compaction and affect its long-term storage capacity, in whatever the stress state (isotropic or deviatoric). Hangx *et al.,* [13] performed conventional triaxial creep experiments, combined with fluid flow-through experiments (brine and $CO_2$-rich brine) on carbonate- and quartz-cemented Captain Sandstone from the Goldeneye field. The carbonate cement dissolution effects on mechanical and ultrasonic properties, as well as on the failure strength of the sandstone were studied. Guen [14] conducted experiments on low and high $P_{CO_2}$ (8 MPa) aqueous fluids injection tests. Fluids exiting the triaxial cells were continuously collected and their compositions analyzed. Results show that all samples showed a positive correlation between fluid flow rate and strain rate. Hangx *et al.,* [13] conducted the test under in situ reservoir conditions, the effect of carbonate cement dissolution on mechanical properties of the sandstone were investigated. Gaus [15] investigated the CO2–rock interactions, and identified the main aspects that possibly affect the safety and/or feasibility of the CO2 storage scheme.

Meanwhile, some studies have also been conducted to investigate the chmical solution effects on the mechanical properties of the rock. Grgic *et al.,* [16], used acoustic emission to study the influence of water, oil and alcohol solutions on the macro mechanical properties of sandstone samples. The results show that there is a close relationship between acoustic emission events and the shape of the creep curve. Creep characteristics of micro cracks can be revealed by studying the static elastic properties of rocks. Chai *et al.*, [17] immersed clayey rocks into different chemical solutions and observed that the expansion effect of clayey rocks relies on the concentration of aqueous solution and the expansion effect decrease with the increase of concentration of the solution. Carrying out uniaxial tests on chemical corroded limestone samples, Feng *et al.*, [15] studied the coupling effect of multiple cracks propagation law and found that the crack evolution of

the chemical corroded samples during the uniaxial loading is very complex, which depends on the pH value of the chemical solution, concentration of chemical ions in solution, mineral composition of the rock and pre-existing cracks, *etc*. Mohtarami *et al.,* [18] used extended finite element method (XFEM) to model fracturing graded brittle rocks by chemical corrosion, and investigated the crack propagation by considering different corrosive solutions under various mechanical loading in three-point and four-point bending tests both numerically and experimentally.

However, the existing studies so far have been mainly focusing on the macro and mesoscopic mechanical properties of rock under the chemical environment, such as the degradation of rock strength and elastic modulus, macro crack propagation, expansion effect of rocks, fracture toughness, *etc*. Under the effect of chemical solutions, large changes would occur at micro scale within rocks. Microstructural changes can cause macro-mechanical changes [19]. Thus, the study on micro damage and mechanical property degradation of chemical corroded rocks is of great importance. However, there is little research on this issue, and thus the prediction of the mechanical behaviour of chemical corroded rocks and effective coupled chemical-mechanical modeling become very difficult.

Various characterization techniques have been proposed to study the change of mechanical properties of rock after chemical erosion, including computerized tomography (CT) technique [20, 21] and Nuclear Magnetic Resonance (NMR) [22, 23]. The NMR is powerful for investigating micro changes inside the samples in great details and also has wide applications in medical diagnosis, geotechnical engineering, oil and gas exploration, and recently in rock tests [24-27]. Li *et al.,* [28] used NMR to investigate the pore structure of the rock. Cai *et al.,* [2] investigated the changes of properties and mechanical characteristics of the rock after chemical erosion under identical loading conditions, including deformation and strength characteristics. Carpenter [29] used NMR imaging to the measurement of water content distributions in limestone. The hydraulic diffusivity of limestone is found to be an approximately exponential function of the water content, in agreement with experimental data on other porous materials.

By using NMR, this paper presents experimental research on the micro damage evolution of limestone treated with different chemical solutions over different immersion periods. NMR images and $T_2$ values (transverse relaxation time distribution which depends on the size of water-saturated pores) for limestone inner sections are obtained. Based on the experimental data, the micro damage evolution is investigated, and the compression stage, micro damages emergence stage, micro damages development stage, fracture and collapse stage of the chemical corroded limestone samples at different loading levels have been obtained and analysed. The influence and relationship between chemical solutions on porosity change as well as the degradation of macro mechanical

3

properties of the limestone samples are summarised. These results will uncover the root reason for changes in mechanical properties of the chemical corroded sedimentary rocks, such as limestone, and reveal the influence of the chemical erosion on micro damage evolution of the rocks under triaxial compression.

## 2 Tested materials and experimental methods

### 2.1 Sample preparation

Sedimentary rock, such as sandstone and limestone, distributes extensively in the superficial lithosphere, which is the main place for underground constructions and engineering geological. Thus, limestone, a common sedimentary rock in southwest China, is selected as the test sample in this experiment. The limestone blocks, which are selected from a single block without macroscopic cracks from a tunnel construction site in Chongqing, are machined into cylindrical shapes with a length of 100 mm and a diameter of 50 mm. By X-ray diffraction (XRD) analysis it is found that the limestone samples are composed of 90% calcspar, quartz, cements and 1% accessory minerals. The microstructure of the limestone is oolithic, as shown in Fig.1.
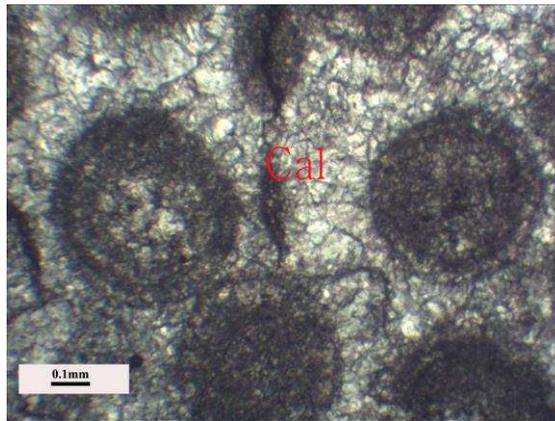


Fig.1. Microscope image of a limestone sample: Cal, calcspar.

### 2.2 Chemical solutions

According to water sample analysis, which is collected from the tunnel construction site in Chongqing, the pH value of the water sample is 6.5 and the main icons are $Na^+$, $Ca^{2+}$, $Mg^{2+}$, $SO_4^{2-}$, $Cl^-$ and $HCO^-$. To simplify the experimental study, the complex ionic composition of the water is replaced by $Na_2SO_4$ solution, which is made by NaCl solution added with $H_2SO_4$. There are three pH values (3, 5 and 7) of the $Na_2SO_4$ solution, and all initial concentrations of the chemical solutions are 0.01 $mol \cdot L^{-1}$.

### 2.3 Testing process

The samples are saturated using a vacuum saturation device. After saturation for 24h, samples with similar initial porosity are selected using NMR and categorised into six groups to be immersed in distilled water and $Na_2SO_4$ solutions with three pH values (3, 5 and 7) for three designed periods (20d, 40d and 60d), as listed in Table 1.

Table 1 Groups of limestone specimens

| No. of specimen | pH | Time/d | No. of specimen | pH | Time/d |
|---|---|---|---|---|---|
| A-1 | 3 | 20 | C-1 | 3 | 60 |
| A-2 | 5 | 20 | C -2 | 5 | 60 |
| A-3 | 7 | 20 | C -3 | 7 | 60 |
| B-1 | 3 | 40 | D-1 | Distilled Water | 20 |
| B -2 | 5 | 40 | D-2 | Distilled Water | 40 |
| B -3 | 7 | 40 | D-3 | Distilled Water | 60 |

When the samples reach the designed erosion period, NMR test is conducted to analyse the porosity change. After the NMR tests, the samples are taken out of the NMR machine and put into the triaxial pressure cell of the Rock 600-50 test system for triaxial compression tests. The confining pressure is gradually increased up to 10 MPa and then fixed. After that, a strain control mode is used for the axial loading at a rate of 0.02 mm·min$^{-1}$ until the sample is ruptured.

After the chemical corrosion, the porosity and skeleton structure of the rock may largely change, which could influence the micro damage evolution of the rock under mechanical loading. Thus, it is necessary to study the micro damage evolution of the chemical corroded rock samples during triaxial compression. In this study, the porosity changes associated with strength degradation are investigated for a series of limestone samples under different triaxial loading stages. The designed loading stage (DLS) of rock can be defined in Equation (1), in which $\sigma_s$ is the peak strength of the initial samples and $\sigma_i$ is a test designed percentage of $\sigma_s$.

$$DLS = \frac{\sigma_i}{\sigma_s} \times 100\% \qquad （1）$$

Sixteen limestone samples are divided into four groups (E-H), with four specimens in each group. These limestone samples are immersed in different pH values solutions for 60 days. After that, samples are loaded to approximately 20%, 40%, 60% and 80% of the peck strength (determined from group C specimens), respectively. These partially loaded samples are removed from the Rock

Testing System and saturated under a vacuum for at least 3 h and their porosities are determined by NMR again. Finally the same samples are tested to failure. Groups of samples are listed in Table 2. It should be noted some cracks produced in mechanical tests may close after the sample is removed from the mechanical machine, but this is not considered in this study.

Table 2 Group of DLS specimens

| No. of specimen | pH | Time / d | DLS/% | No. of specimen | pH | Time / d | DLS/% |
|---|---|---|---|---|---|---|---|
| E-1 | 3 | 60 | 20 | G-1 | 7 | 60 | 20 |
| E-2 | 3 | 60 | 40 | G-2 | 7 | 60 | 40 |
| E-3 | 3 | 60 | 60 | G-3 | 7 | 60 | 60 |
| E-4 | 3 | 60 | 80 | G-4 | 7 | 60 | 80 |
| F-1 | 5 | 60 | 20 | H-1 | Distilled Water | 60 | 20 |
| F-2 | 5 | 60 | 40 | H-2 | Distilled Water | 60 | 40 |
| F-3 | 5 | 60 | 60 | H-3 | Distilled Water | 60 | 60 |
| F-4 | 5 | 60 | 80 | H-4 | Distilled Water | 60 | 80 |

## 3 Experimental results

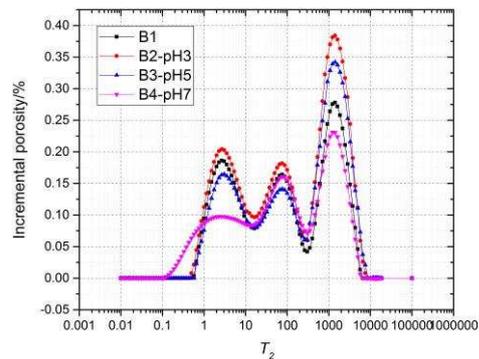### 3.1 NMR $T_2$ spectrum distribution

NMR is a process in which the nuclei in a magnetic field absorb and re-emit electromagnetic radiations. During rock NMR porosity measurement, NMR machine mainly detects the NMR signal of the hydrogen nucleus (1H) from fluids within the rock pores. Thus, when rock is saturated with water, the detected signal is proportional to the pore volume. By measuring the signal intensity of the hydrogen atoms of the water in the fully-saturated rock, NMR system outputs transverse relaxation time distribution ($T_2$ spectrum), which can be converted to a pore size distribution. The signal strength of the $T_2$ spectrum depends on the size of water-saturated pores. The area between the curve and horizontal axis is $T_2$ spectrum area, which has a close relationship with porosity and pore size distribution of the rock, and can be convert to porosity of the sample by NMR machine, *i.e.*, the porosity increases with the $T_2$ spectrum area and the peak point of the curve increases when the pore size increase.

$T_2$ spectrum of limestone immersed in distilled water and different pH values chemical solutions over different periods are shown in Fig.2. The $T_2$ spectrum distribution for limestone sample has three peaks. The left peak and the middle peak indicate the small pores and the third one indicates bigger pores. A few observations can be made from the test results shown in Fig.2: After limestone samples being immersed in chemical solution or distilled water, there is an increase of the $T_2$ spectrum area and a noticeable change of curve shape, indicating an increased porosity; The largest change of $T_2$ spectrum is found in samples immersed in solution with pH3 values, while the smallest spectrum change belongs to the sample immersed in distilled water. This is because calcspar in the limestone samples reacts with $H^+$ ions in acidic solution, which causes new small pores and promotes larger pores to form. For the samples immersed in distilled water, some of the minerals in the limestone dissolve when immersed in water, leading to the formation of small pores and the enlargement of pores, but the porosity changes are slighter compared to samples immersed in pH3 solutions.
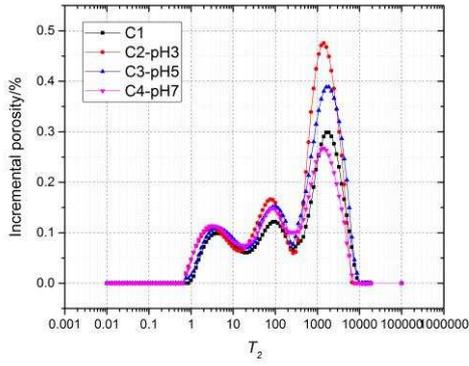
After immersed in chemical solutions and distilled water for 20 days, as shown in Fig.2 (a), there are significant changes in the second and third peaks. That indicates the pore size expands and the number of large pores increases. Figure 5(b) and 5(c) shows the $T_2$ spectrum of the samples immersed in solution for 40 days and 60 days. There are significant changes in the second and third peaks. This indicates there is an increase in small pores, some of which become interconnected to form larger pores. This is due to the fact that with an increase in immersion time in the chemical environment, the acid solution continuously permeates the limestone samples, forming new microscopic pores and expanding small pores. Furthermore, the changes observed in pH7 solution and distilled water are less obvious than that in pH3 environment.
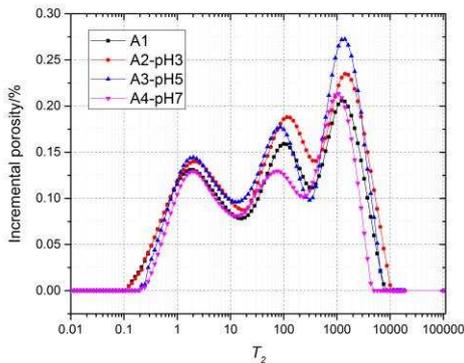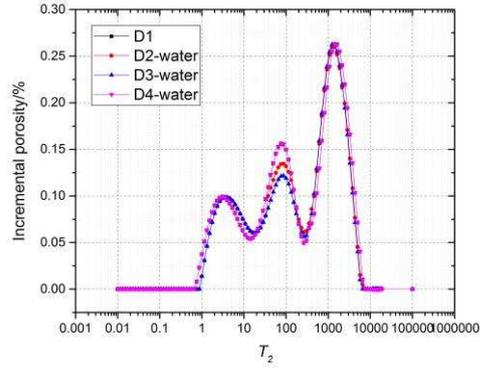


(a) $T_2$ spectrums of samples immersed in $Na_2SO_4$ for 20 days      (b) $T_2$ spectrums of samples immersed in $Na_2SO_4$ for 40 days
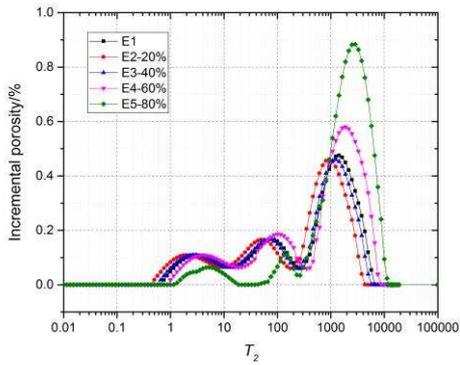
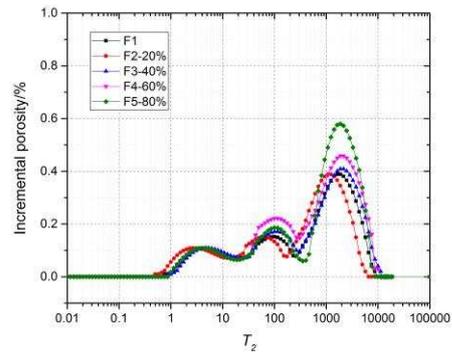(c) $T_2$ spectrums of samples immersed in $Na_2SO_4$ for 60 days    (d) $T_2$ spectrums of samples immersed in distilled water

Fig.2. $T_2$ spectrum distribution of limestone in different chemical solutions after different days of soaking.

After being immersed in chemical solutions for 60 days, samples from the groups E-H are designed to be compressed approximately 20%, 40%, 60% and 80% of the peak strength of group C, and then NMR is used to measure damage change after the triaxial compression tests. $T_2$ spectrum results of these samples are shown in Figure 6.



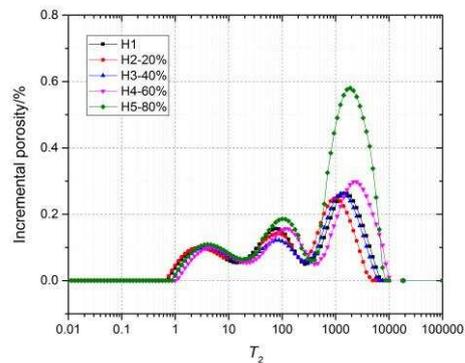(a) $T_2$ spectrums of samples immersed in $Na_2SO_4$ for 20 days    (b) $T_2$ spectrums of samples immersed in $Na_2SO_4$ for 40 days



(c) $T_2$ spectrums of samples immersed in $Na_2SO_4$ for 60 days    (d) $T_2$ spectrums of samples immersed in distilled water

8
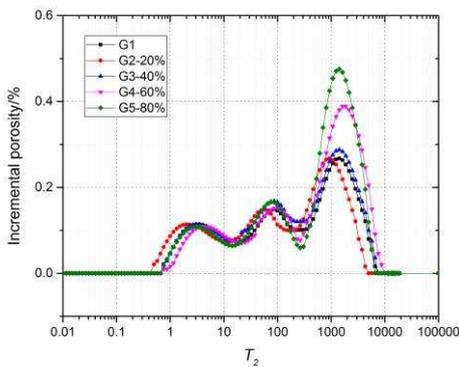
Fig.3. Comparison of $T_2$ pore size distribution in specimens under pre- and post-loading conditions.

Overall, Fig.3(a)-(d) indicate that the number and size of micro-cracks in specimens increase with the increase of triaxial compression. From the test results, it can be found that: When the axial compression ratio is about 20%-40%, there are slightly decreases in the first and third peaks due to the fact that the specimens are compacted; When the axial compression ratio is about 40%-80%, the first and second peak of $T_2$ spectrum is bigger, which means the micro damage of limestone rock mass is caused by sharp increase of micro cracks by both number and size; When the axial compression ratio is 80%, third peak of $T_2$ spectrum increases a lot, which indicate there are large amount of bigger micro cracks due to coalesce. As the axial loading continues, the micro cracks inside the limestone samples will sustainably connect to form macro cracks leading to final rupture.

## 3.2 Porosity

Samples with different chemical erosion for NMR investigation of porosity changes are listed Table 3. Fig.4 shows that the porosity generally increases with immersion time, but the increase rate depends on the pH values of solutions.

Table 3 Porosity changes in limestone samples after chemical erosion

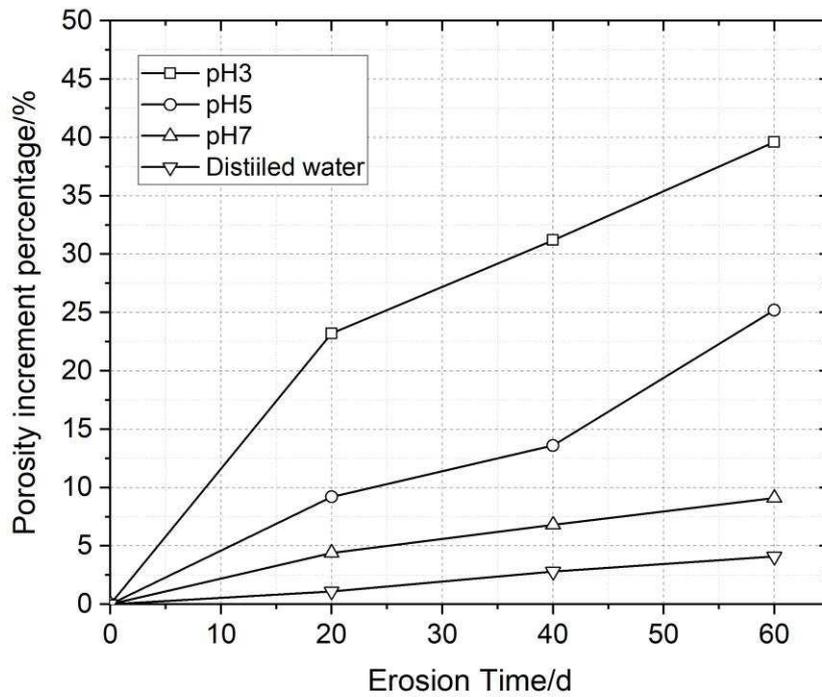| NO of samples | Time/d | pH | Initial Porosity | Erosion Porosity | Porosity Change |
|---|---|---|---|---|---|
| A-1 | 20 | 3 | 5.43 | 6.68 | 23.2 |
| A-2 | 20 | 5 | 5.37 | 5.85 | 9.2 |
| A-3 | 20 | 7 | 5.38 | 5.62 | 4.4 |
| B-1 | 40 | 3 | 5.35 | 7.02 | 31.2 |
| B-2 | 40 | 5 | 5.31 | 6.03 | 13.6 |
| B-3 | 40 | 7 | 5.36 | 5.72 | 6.8 |
| C-1 | 60 | 3 | 5.46 | 7.62 | 39.6 |
| C-2 | 60 | 5 | 5.36 | 6.71 | 25.2 |
| C-3 | 60 | 7 | 5.32 | 5.85 | 9.1 |
| D-1 | 20 | Distilled Water | 5.39 | 5.44 | 1.1 |
| D-2 | 40 | Distilled Water | 5.34 | 5.49 | 2.8 |
| D-3 | 60 | Distilled Water | 5.33 | 5.54 | 4.1 |

Fig.4. Porosity changes in limestone samples after immersion in chemical solutions.

After immersion, the porosity increase more or less linearly against immersion period. In addition, solution with a lower pH value gives a higher rate of porosity change due to more intense chemical reaction, and the samples immersed in distilled water show the smallest increase in porosity, *i.e.*, 4.1%.

The changes of the limestone in microscopic are resulted from the chemical reactions taking place inside the limestone samples, such as calspar and the micro-calcite react with $H^+$ ions, which lead to porosity increasing. Due to chemical ions exchange between the solution and the rock [30], there is a slight increase of porosity of the samples corroded by pH7 solution, and the porosity growth is higher than that in distilled water. The porosity increment is the smallest in the distilled water among all the sample groups. While the porosity increase of limestone samples immersed in distilled water is relatively smaller. This is because the microstructual change of limestone samples exposed to distilled water is mainly caused by the softening of the rock as well as the dissolution of some dissolved minerals and calcite dissolution, since the distilled water is not chemically balanced with the immersed limestone samples, but there has not been a more violent chemical reaction of the samples immersed in pH7 solution and distilled water.

Generally, the volume of micro-pores of rocks increase gradually as higher loads applied, which is indicated by Table 4 and Fig.5. When the axial compression ratio is about 20% and 40%, porosity

10

of sample E-1 and E-2 (samples immersed in pH3 $Na_2SO_4$ solution) decrease slightly to 7.35% and 7.55% respectively, which is lower than the one with no loading, 7.62%. This indicates samples E-1 and E-2 are compressed. However, during the same period, porosity of samples G-1 and G-2 (samples immersed in pH7 $Na_2SO_4$ solution) is 5.72% and 6.26%, whilst the porosity of the sample with no loading is 5.85%. This indicates that the limestone samples immersed in lower pH solutions has a longer compression stage. This is because lower pH values solution increase the porosity of limestone samples significantly regards to other groups of samples. High porosity would enlarge the compression stage.

When the axial compression ratio is about 40%-60%, the samples perform elastic deformation and the increase of porosity is small. When the axial compression ratio is above 60% and below 80%, plastic deformation occurs and the porosity of samples increases significantly, such as samples in group E, which porosity increases from 7.55% to 8.74%.

Table 4 Porosity changes in limestone samples under different loading conditions

| DLS/% | pH-3 | pH-5 | pH-7 | Distilled Water |
|---|---|---|---|---|
| 0 | 7.62 | 6.71 | 5.85 | 5.54 |
| 20 | 7.35 | 6.56 | 5.72 | 5.42 |
| 40 | 7.55 | 6.93 | 6.26 | 5.77 |
| 60 | 8.74 | 7.49 | 6.91 | 6.15 |
| 80 | 10.15 | 8.92 | 7.71 | 7.23 |
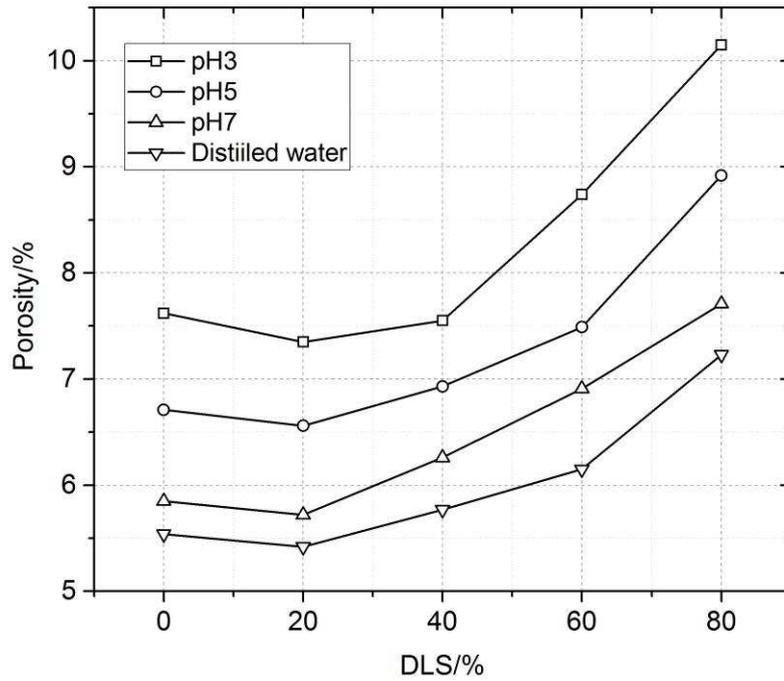
Fig.5. Porosity changes in limestone samples after compression

## 3.3 Peak strength and Young modulus

The chemical solutions have an impact on microstructure of limestone as well as the mechanical properties. Fig.6 shows that the peak strength of limestone samples from group A to group D with different immersion time. Fig.7 shows the elastic moduli of limestone samples immersed in different chemical solutions for different periods of time.

Fig.6. Peak strength of limestone immersed in different chemical solutions



Fig.7. Young modulus of limestone soaked in different chemical solutions.

## 4 Chemical effects and micro damage evolution

## 4.1. Corrosion mechanisms

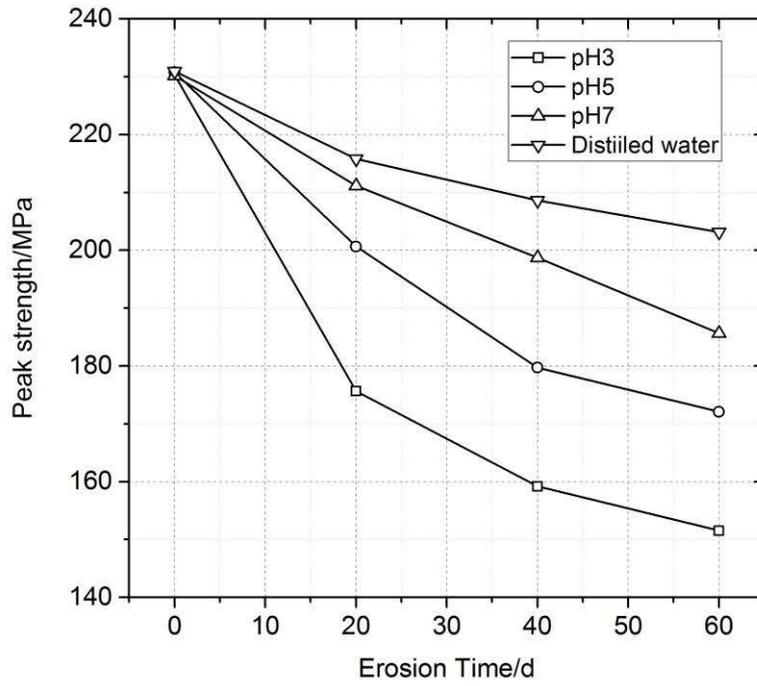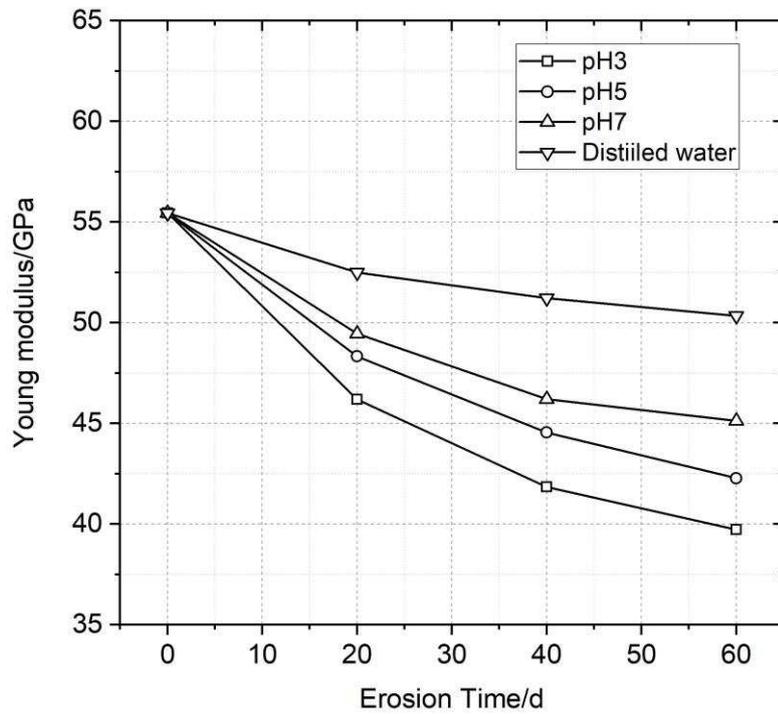Rock material is a complex medium often containing many chemical ions. Due to the geological processes, underground rock is always surrounded by water and contains many pre-existing internal micro-cracks. Therefore, the rock is unavoidably permeated by water and reacts with the chemical icons in the water. These chemical erosions would change the microstructure of the rock,

Two factors have contributed to the changes in the composition and porosity of rock. First, there is dissolution. Some mineral particles in the rock in contact with water will dissolve. Second, there are chemical reactions, which means some mineral in rock react easily with chemical ions in chemical solution. These two factors lead to an increase in porosity, weaken the skeleton of the rock and form new minerals of the rock, which eventually lead to the degradation of its macro mechanical properties [31, 32].

Mineral compositions in different rocks are different, which means that chemical corrosion effects also differ. According to the mineral tests, the limestone samples in this test are mainly composed of oolite, calcspar, quartz, cement, bio clastic and metal minerals. The calcspar in the limestone samples can easily react with acid ions (*e.g.* $H^+$), resulting an increase of the porosity. Moreover, the cement is soluble in water, causing secondary porosity, as well as changes in the rock structure,

Calcspar and the micro-calcite undergoes a certain degree of dissolution and hydrolysis in the chemical environment. The following reactions are likely to occur in an acidic solution：

$$CaCO_3 + 2H^+ \rightarrow Ca^{2+} + H_2O + CO_2 \uparrow \qquad (2)$$
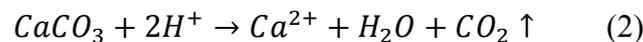
The reaction of iron oxide is:

$$Fe_2O_3 + 6H^+ \rightarrow 2Fe^{3+}3H_2O \qquad (3)$$
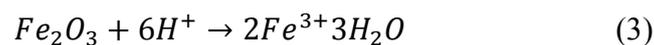
The main mineral composition of quartz is $SiO_2$, which is stable in acidic and neutral environments. The reaction in distilled water is:

$$SiO_2 + 2H_2O \rightarrow H_4SiO_4 \qquad (4)$$
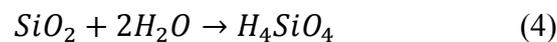
Formulas (4)–(6) show that limestone samples in this study undergoes different reactions in chemical environments, resulting in various degrees of porosity changes and skeleton softening.

Fig.8 illustrates the relationship between the porosity increase and peak strength of the treated limestone samples, and Fig.9 illustrates that the relationship between the porosity increase and elastic modulus of the treated limestone samples. All the mechanical properties decrease with the increasing of porosity. The largest reduction of mechanical properties is found in the limestone samples in pH3 solution, and the degree of chemical corrosion is smallest in the distilled water.
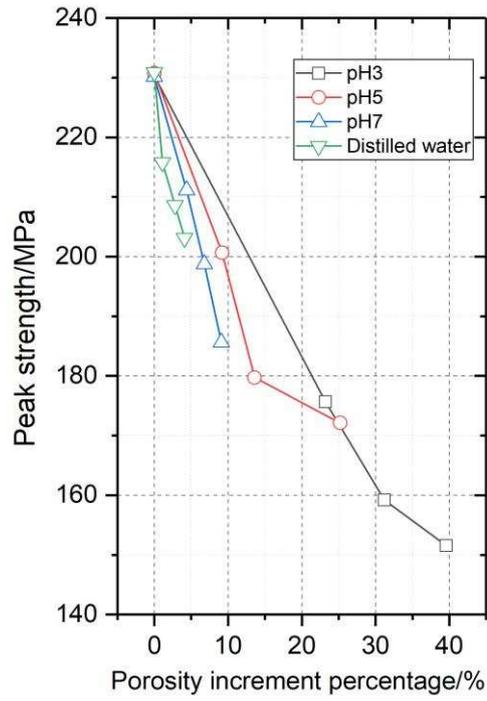
Fig.8. Percentage of porosity increment vs peak strength of the limestone samples
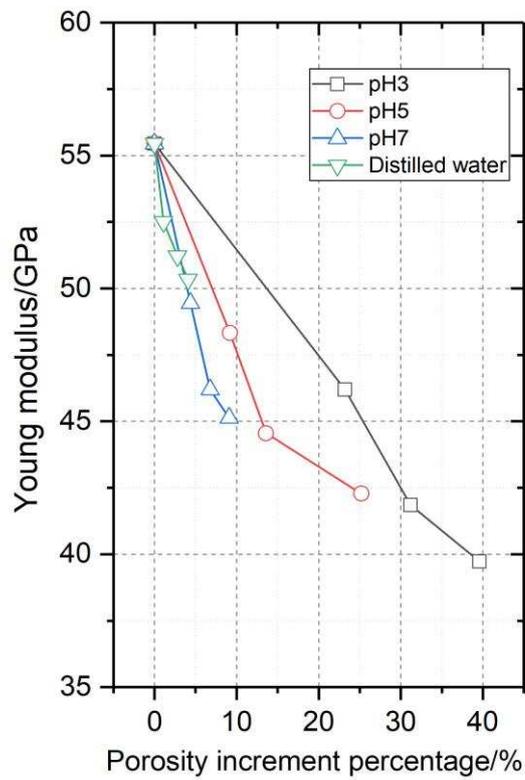
Fig.9. Percentage of porosity increment vs young modulus of the limestone samples
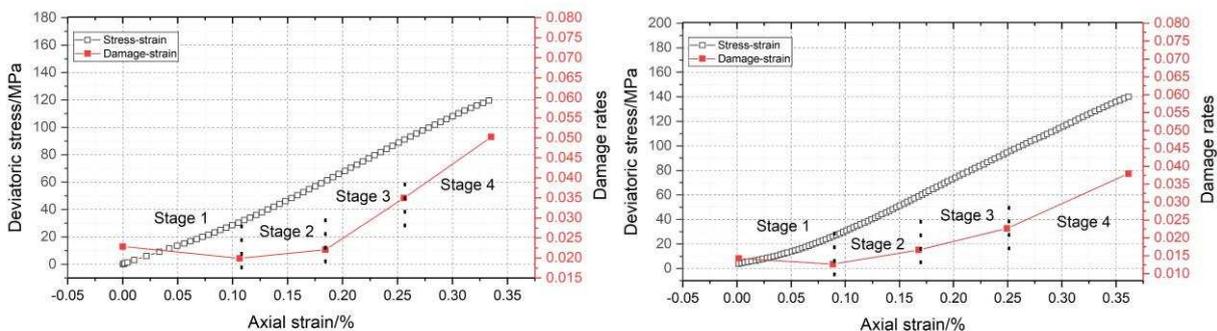
## 4.2 Micro damage propagation under external stress

Different parameters have been chosen to calculate micro damage, which include Elastic modulus [33], strain rates [34], Energy dissipation [35], Ultrasonic wave velocity[36, 37], and A reasonable damage variable must meet the basic requirements: it could take the initial damage into consideration; it is easy to be measured and calculated; its evolution law can reflect the real micro damage of the rock; it has actual physical meaning [38]. For the limestone samples corroded by chemical solution, the change of porosity is the root cause of macro mechanical properties degradation. Furthermore, as the initial porosity can be obtained by NMR, the pre-existing damage can be taken into account in this method. Therefore, porosity is used as a damage variable in this study to reflect the degree of corrosion in different chemical solutions.

The chemical damage variables are calculated as [39]:

$$D = \frac{V - V_D}{V} = \frac{n - n_0}{1 - n_0} \qquad (5)$$

Where $D$ is the damage variable after t days immersion, $n_0$ is the porosity of the original sample, and $n$ is the porosity after immersion for $t$ days. Therefore, the damage evolution process of the limestone samples treated with chemical erosion and different loading condition can be studied.

The micro damage of limestone is calculated according to the porosity changes according to formula (5). The micro damage of the key loading points is selected in this test, 20%, 40%, 60%, 80% of the peak strength. The micro damage-stress-strain relationship curves of the corroded sample under external stress are presented in Fig 8. The MRI (Magnetic Resonance Imaging, obtained by NMR system) of the sample is also presented in Fig 8. The white points in the MRI reflect the water inside the rock and the black area is the background. The brightness and the number of white points of the image increase when the porosity increases.

(c) Group G (pH7 solution for 60days)　　　　(d) Group H (distilled water for 60days)

Fig.9. (a-d) NMI, micro damage-strain and stress-strain curves of the limestone samples.

It is shown that the micro damage increase and the NMR image become brighter with the increase of stress, and the micro damage of samples immersed in pH3 solutions often grow faster than that in other solutions. Above all, the micro damage law of limestone samples subjected to different compression loads can be divided into four stages: compression stage, micro damages emergence stage, stage of micro damages development, fracture and collapse stage. Under the external stress, the limestone samples are firstly compacted and the micro crack and pores are closed, so that the damage rate decreases. After that, the number of small pores increases, some of these pores become interconnected, forming larger pores. When the loading stress reaches a certain point, which will be shown later, the micro cracks increasing rate is reduced and the micro cracks are connected into macro fracture zones, which leads to rupture of the limestone samples.
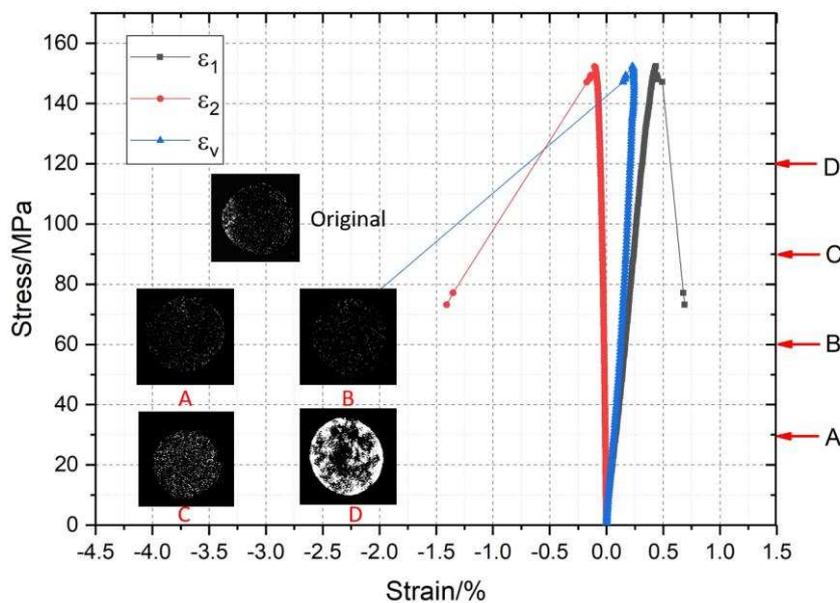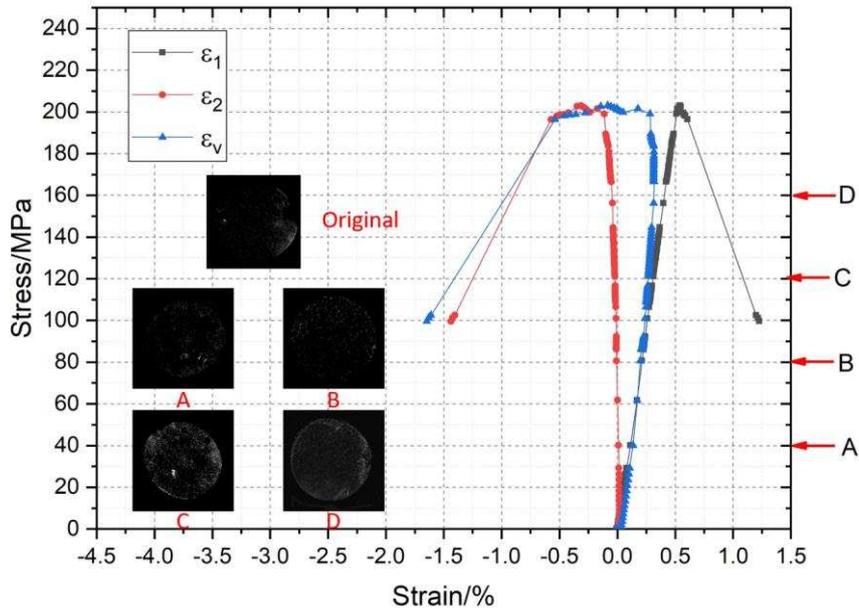
(b) Sample immersed in distilled water

Fig.11 MRI and stress-strain curve of the limestone sample (Point A: 20%of the peak strength, Point B: 40%of the peak strength, Point C: 60%of the peak strength, Point D: 80%of the peak strength.)

The length of those damage stages has a close relationship with the damage caused by chemical solutions erosion, which makes the length of each micro damage stage is different in each group. The compression stage of limestone samples immersed in lower pH3 solution is longer than that in higher pH values solution and distilled water. And the samples immersed in pH3 values solution, the micro damages development stage is shorter than that immersed in distilled water. This is because the rock structure of limestone samples after chemical erosion becomes softer than the original ones, which makes the damage evolution process accelerated. This is different from the micro damage evolution process of the samples immersed in distilled water, in which micro damages development stage is slowly developed relatively. In conclusion, the chemical erosion accelerates the convergence of the micro crack as well as the rupture stage.

Take Group E (samples immersed in pH3 values solution) and Group H (samples immersed in distilled water) as an example, which is shown in Fig.9. When the loading stress in Group E reaches 30.31 MPa (20% of the peak strength of C-1, which is 151.55 MPa), the damage rate decreases slightly from 0.0228 to 0.0199. This means that the internal micro-cracks and are closing up, and the sample is compressed. This can also be observed from the NMR images, which become darker. When the loading stress reaches 60.62 MPa (40% of the peak strength of C-1), the damage rate

increases slightly from 0.0199 to 0.0220 but still lower than the original sample C-1, which indicates the sample is still in compression stage. However, when the loading stress of sample H reaches 40% of the peak strength, the damage rate begins to increase from 0.0009 to 0.0046. This means that the internal micro-cracks are emerging and the sample in group H already reaches micro damages emergence stage. Compared with $T_2$ values in Fig. 6, when the loading stress of sample in group E reaches 60% of the peak strength, the first and third peaks increase, indicating that the number of small pores increases and some of them become interconnected to form larger pores as the samples are in sustainable development stage. However, during the same period, the samples in Group H are still in micro damages emergence stage.

Furthermore, for chemical corroded samples, when the axial compression ratio is below 80%, the micro damage of limestone rock mass is caused by a sharp increase of number and size of micro cracks. However, when the axial compression ratio is above 80%, the samples reach fracture and collapse stage. In this stage, the micro cracks increasing is restrained, the micro damage of limestone rock mass is caused by micro crack connection.

## 5 Conclusions

With the application of NMR technique, this study investigated the porosity changes of limestone after chemical erosion, and analysed the relationship between chemical erosion and the micro crack propagation during triaxial compression. Based the experiments, some conclusions can be drawn as following:

(1) The NMR technique has been found to be successful for investigating the micro damage evolution of limestone under chemical erosion and triaxial mechanical loading. The micro cracks in limestone samples treated with different pH values of chemical solutions and under different loading conditions can be directly visualised by the NMR system.

(2) By using the NMR, the $T_2$ values, NMR images are obtained, and result indicates that the porosity change is the root cause of the mechanical properties degradation. Meanwhile, by choosing porosity as the micro damage variable, the internal rock damage evolution process can be calculated, formula (3).

(3) Chemical corrosion changes the mechanical properties of the limestone samples, and the micro damage evolution law of limestone samples subjected to different compression loads can be divided into four stages: compression stage, micro damages emergence stage, stage of micro damages development, fracture and collapse stage. The characters of these stages, which are investigated by NMR experiments, have a close relationship with the chemical induced micro damage.

(4) Based on the experimental results, the chemical-mechanical modeling will be pending for further research, and the results can be used for prediction of the mechanical behaviour of chemical corroded rocks in real constructions.

## Acknowledgements

## Reference

[1]STEEFEL, C. I. & VAN CAPPELLEN, P. A new kinetic approach to modeling water-rock interaction: The role of nucleation, precursors, and Ostwald ripening[J]. Geochimica et Cosmochimica Acta. 1990, 54(10):2657-2677.

[2]CAI, Y.-Y., YU, J., FU, G.-F. & LI, H. Experimental investigation on the relevance of mechanical properties and porosity of sandstone after hydrochemical erosion[J]. Journal of Mountain Science. 2016, 13(11):2053-2068.

[3]CHAI, Z.-Y., KANG, T.-H. & FENG, G.-R. Effect of aqueous solution chemistry on the swelling of clayey rock[J]. Applied Clay Science. 2014, 93:12-16.

[4]CROIZÉ, D., BJØRLYKKE, K., JAHREN, J. & RENARD, F. Experimental mechanical and chemical compaction of carbonate sand[J]. Journal of Geophysical Research: Solid Earth. 2010, 115(B11).

[5]ALONSO, E., ZANDARÍN, M. & OLIVELLA, S. Joints in unsaturated rocks: thermo-hydro-mechanical formulation and constitutive behaviour[J]. Journal of Rock Mechanics and Geotechnical Engineering. 2013, 5(3):200-213.

[6]BEN ABDELGHANI, F., AUBERTIN, M., SIMON, R. & THERRIEN, R. Numerical simulations of water flow and contaminants transport near mining wastes disposed in a fractured rock mass[J]. International Journal of Mining Science and Technology. 2015, 25(1):37-45.

[7]LA FELICE, S., MONTANARI, D., BATTAGLIA, S., BERTINI, G. & GIANELLI, G. Fracture permeability and water–rock interaction in a shallow volcanic groundwater reservoir and the concern of its interaction with the deep geothermal reservoir of Mt. Amiata, Italy[J]. Journal of Volcanology and Geothermal Research. 2014, 284:95-105.

[8]GAUS, I., AZAROUAL, M. & CZERNICHOWSKI-LAURIOL, I. Reactive transport modelling of the impact of $CO_2$ injection on the clayey cap rock at Sleipner (North Sea)[J]. Chemical Geology. 2005, 217(3):319-337.

[9]PORTIER, S. & ROCHELLE, C. Modelling $CO_2$ solubility in pure water and NaCl-type waters from 0 to 300 °C and from 1 to 300 bar: Application to the Utsira Formation at Sleipner[J]. Chemical Geology. 2005, 217(3):187-199.

[10]ASSAYAG, N., MATTER, J., ADER, M., GOLDBERG, D. & AGRINIER, P. Water–rock interactions during a $CO_2$ injection field-test: Implications on host rock dissolution and alteration effects[J]. Chemical Geology. 2009, 265(1):227-235.

[11]GOLUBEV, S. V., BÉNÉZETH, P., SCHOTT, J., DANDURAND, J. L. & CASTILLO, A. Siderite dissolution kinetics in acidic aqueous solutions from 25 to 100 °C and 0 to 50 atm $pCO_2$[J]. Chemical Geology. 2009, 265(1):13-19.

[12]GRGIC, D. Influence of $CO_2$ on the long‐term chemomechanical behavior of an oolitic limestone[J]. Journal of Geophysical Research: Solid Earth. 2011, 116(B7).

[13]HANGX, S., VAN DER LINDEN, A., MARCELIS, F. & BAUER, A. The effect of CO2 on the mechanical properties of the Captain Sandstone: Geological storage of CO2 at the Goldeneye field (UK)[J]. International Journal of Greenhouse Gas Control. 2013, 19:609-619.

[14]LE GUEN, Y., RENARD, F., HELLMANN, R., BROSSE, E., COLLOMBET, M., TISSERAND, D. & GRATIER, J. P. Enhanced deformation of limestone and sandstone in the presence of high fluids[J]. Journal of Geophysical Research: Solid Earth. 2007, 112(B5).

[15]GAUS, I. Role and impact of CO2–rock interactions during CO2 storage in sedimentary rocks[J]. International Journal of Greenhouse Gas Control. 2010, 4(1):73-89.

[16]GRGIC, D. & GIRAUD, A. The influence of different fluids on the static fatigue of a porous rock: Poro-mechanical coupling versus chemical effects[J]. Mechanics of Materials. 2014, 71:34-51.

[17]CHAI, Z.-Y., KANG, T.-H. & FENG, G.-R. Effect of aqueous solution chemistry on the swelling of clayey rock[J]. Applied Clay Science. 2014, 93-94:12-16.

[18]MOHTARAMI, E., BAGHBANAN, A., EFTEKHARI, M. & HASHEMOLHOSSEINI, H. Investigating of chemical effects on rock fracturing using extended finite element method[J]. Theoretical and Applied Fracture Mechanics. 2017, 89:110-126.

[19]SETO, M., NAG, D. K., VUTUKURI, V. S. & KATSUYAMA, K. Effect of chemical additives on the strength of sandstone[J]. International Journal of Rock Mechanics and Mining Sciences. 1997, 34(3):280.e1-280.e11.

[20]GE, X., REN, J., PU, Y., MA, W. & ZHU, Y. Real-in time CT test of the rock meso-damage propagation law[J]. Science in China Series E: Technological Sciences. 2001, 44(3):328-336.

[21]FENG, X. T., CHEN, S. L. & ZHOU, H. Real-time computerized tomography (CT) experiments on sandstone damage evolution during triaxial compression with chemical corrosion[J]. International Journal of Rock Mechanics and Mining Sciences. 2004, 41(2):181-192.

[22]ADEBAYO, A. R., KANDIL, M. E., OKASHA, T. M. & SANNI, M. L. Measurements of electrical resistivity, NMR pore size and distribution, and x-ray CT-scan for performance evaluation of CO2 injection in carbonate rocks: A pilot study[J]. International Journal of Greenhouse Gas Control. 2017, 63:1-11.

[23]LI, J.-L., ZHOU, K.-P., LIU, W.-J. & DENG, H.-W. NMR research on deterioration characteristics of microscopic structure of sandstones in freeze–thaw cycles[J]. Transactions of Nonferrous Metals Society of China. 2016, 26(11):2997-3003.

[24]YAO, Y. & LIU, D. Comparison of low-field NMR and mercury intrusion porosimetry in characterizing pore size distributions of coals[J]. Fuel. 2012, 95:152-158.

[25]ZHOU, K.-P., BIN, L., LI, J.-L., DENG, H.-W. & FENG, B. Microscopic damage and dynamic mechanical properties of rock under freeze–thaw environment[J]. Transactions of Nonferrous Metals Society of China. 2015, 25(4):1254-1261.

[26]SØRLAND, G. H., DJURHUUS, K., WIDERØE, H. C., LIEN, J. R. & SKAUGE, A. Absolute pore size distributions from NMR[J]. Diffusion Fundamentals. 2007, 5:4.1-4.15.

[27]SCHOENFELDER, W., GLÄSER, H.-R., MITREITER, I. & STALLMACH, F. Two-dimensional NMR relaxometry study of pore space characteristics of carbonate rocks from a Permian aquifer[J]. Journal of Applied Geophysics. 2008, 65(1):21-29.

[28]LI, H.-B., ZHU, J.-Y. & GUO, H.-K. Methods for calculating pore radius distribution in rock from NMR T2 spectra[J]. Chinese Journal of Magnetic Resonance. 2008, 2:017.

[29]CARPENTER, T. A., DAVIES, E. S., HALL, C., HALL, L. D., HOFF, W. D. & WILSON, M. A. Capillary water migration in rock: process and material properties examined by NMR imaging[J]. Materials and Structures. 1993, 26(5):286.

[30]REVELLE, R. & EMERY, K. O. 1957. Chemical erosion of beach rock and exposed reef rock: Bikini and nearby atolls, Marshall Islands, US Government Printing Office.

[31]LASAGA, A. C. Chemical kinetics of water‐rock interactions[J]. Journal of Geophysical Research: solid earth. 1984, 89(B6):4009-4025.

[32]JEFFERY, P. G. & HUTCHISON, D. 1981. Chemical methods of rock analysis, Pergamon Press Ltd.

[33]AL-SHAYEA, N. A. Effects of testing methods and conditions on the elastic properties of limestone rock[J]. Engineering Geology. 2004, 74(1):139-156.

[34]BAGDE, M. N. & PETROŠ, V. Fatigue properties of intact sandstone samples subjected to dynamic uniaxial cyclical loading[J]. International Journal of Rock Mechanics and Mining Sciences. 2005, 42(2):237-250.

[35]XU, J., YANG, H., LI, S. & JIANG, Y. Experimental study of effects of cyclic loading and unloading pore water pressure on deformation characteristic of sandstone[J]. Chinese Journal of Rock Mechanics and Engineering. 2009, 5:008.

[36]ZHANG, Q.-X., GE, X.-R., HUANG, M. & SUN, H. Testing study on fatigue deformation law of red-sandstone under triaxial compression with cyclic loading[J]. Yanshilixue Yu Gongcheng Xuebao/Chinese Journal of Rock Mechanics and Engineering. 2006, 25(3):473-478.

[37]SONG, H., ZHANG, H., KANG, Y., HUANG, G., FU, D. & QU, C. Damage evolution study of sandstone by cyclic uniaxial test and digital image correlation[J]. Tectonophysics. 2013, 608:1343-1348.

[38]XIAO, J. Q., FENG, X. T., DING, D. X. & JIANG, F. L. Investigation and modeling on fatigue damage evolution of rock as a function of logarithmic cycle[J]. International Journal for Numerical and Analytical Methods in Geomechanics. 2011, 35(10):1127-1140.

[39]KACHANOV, L. M. Rupture time under creep conditions[J]. International journal of fracture. 1999, 97(1-4):11-18.